Supporting Information for:

Photochromic Clock Reaction of Anthraquinone in Supramolecular Gel and Its Application to Spatiotemporal Patterning

Sota Fujisaki[a], Yuki Nagai[a]*, Yoshinori Okayasu[a], Yoichi Kobayashi[a,b]*

a) Department of Applied Chemistry, College of Life Sciences, Ritsumeikan University, 1-1-1 Nojihigashi, Kusatsu, Shiga 525-8577, Japan.

b) PRESTO, JST, 4-1-8 Honcho, Kawaguchi, Saitama 332-0012, Japan

E-mail: ynagai@fc.ritsumei.ac.jp; ykobayas@fc.ritsumei.ac.jp

CONTENTS

General Methods

Materials

Anthraquinone, Boc-l-glutamic acid, 1-hydroxybenzotrizole and triethylamine were purchased from Tokyo Chemical Industry Co. (TCI). Octadecylamine and 1-ethyl-3-(3-dimethylaminopropyl)carbodiimide hydrochloride were purchased from FUJIFILM Wako Pure Chemical Co. Dichloromethane, tetrahydrofuran, methanol, ethanol (95%) and chloroform-d were purchased from Kanto Chemical Co. and were used without further purification.

Nuclear magnetic resonance spectroscopy (NMR):

^{1}H-NMR spectra were measured on an ECZ-400 spectrometer (JEOL, 400 MHz).

Sample preparation:

Typically, anthraquinone (AQ, 400 μM) and triethylamine (TEA, 4 mM) were dissolved in ethanol to give the solution samples. For samples with NaOH, 5 mM NaOH was added to the solution. For the gel sample, the gelator (10.6 mM in the standard condition) was added to the solution and dissolved by heating to 55 °C, and the sol was left at room temperature to give the gel. Bubbling for the gel sample was conducted in the sol state.

For taking images in Fig. 2a, the gels containing 1 mM anthraquinone and 10 mM triethylamine were prepared in the 2-mm quartz cuvette. For the sample with NaOH, 10 mM NaOH was added.

Photoreduction and air-oxidation:

Photoirradiation for photoreduction of the sample in the cuvette was basically conducted by a 365-nm LED light source LC-L1V3 (HAMAMATSU). The light intensity was set to 14.5 mW cm^{-2} except for taking the gel images in the cuvette (Fig. 2a, ~10 mW cm^{-2}) and the light intensity dependence measurement (Fig. 3c, S8). For spatiotemporal patterning experiments, a UV-LED controller CL-1501 (Asahi Spectra) and a 365-nm LED CL-H1-365-9-1-B (Asahi Spectra) equipped with a rod lens RLQL80-1 (Asahi Spectra).

For the solution samples, air-oxidation was conducted by shaking the cuvette. For the gel samples, air-oxidation was conducted by shaking the cuvette in the sol state heated up to 55 °C. In cyclability measurements of the photoreduction (Fig. 2e, S6, S7), air bubbling was conducted to oxidize the reduced form of anthraquinone and to saturate the sample with air.

UV-Vis-NIR absorption spectroscopy:

UV-Vis-NIR spectra were measured on a UV-3600 spectrometer (SHIMADZU). The 1-mm quartz cuvette was used.

Measurements of the time evolution of absorption:

Absorbance change over time was traced using an OCEAN FX spectrometer (Ocean Optics) as a detector and a DH-2000-BAL deuterium-halogen light source (Ocean Optics) as a probe light source. To suppress the effect of probe light on photoreaction, light sources were controlled by a home-made MATLAB code in the following ways: For measurements of coloration dynamics, the probe light and the 365-nm LED light (LC-L1V3, HAMAMATSU) were alternatingly irradiated for 0.1 s and 5 s, respectively. For measurements of decoloration dynamics, the probe

light was irradiated for only 0.1 s per 120 s. The spectral data were acquired during the probe light irradiation. The 1-mm quartz cuvette was used.

Fluorescence spectroscopy:

Fluorescence spectra were measured on an FP-6500 spectrofluorometer (JASCO). The excitation wavelength was 365 nm, and the 1-mm quartz cuvette was used.

Gas composition control:

Two gas flowmeters NFM-V-P-A-500-C (TEHKNE Corporation) were connected to the nitrogen gas line and a diaphragm pump discharging the air, respectively. The flow-regulated nitrogen and air were mixed using a T-shaped tube, and the mixed gas was used for the bubbling operation. The volume fraction of oxygen in the mixed gas was calculated, assuming the oxygen volume fraction in the air is 0.21.

Microsecond transient absorption spectroscopy:

Microsecond transient absorption measurements were conducted using a TSP–2000 time-resolved spectrophotometer (Unisoku). The third harmonics (355 nm) of a 10 Hz Q–switched Nd:YAG laser (Continuum Minilite II) (ca. 1 mJ per 5 ns pulse) were used as the excitation light. To minimize the effect of the probe light on photoreaction, the probe light intensity was weakened as possible. The measurements were performed for an ethanol solution of anthraquinone (400 μM) and triethylamine (4 mM) placed in the 1-cm quartz cuvette at room temperature.

Spatiotemporal photopatterning:

The photomask was fabricated by printing with black ink on an overhead projector film made of polyester (Fig. S14). The transmittance of each part of the photomask was determined from the 365-nm LED intensities measured by an optical power meter; the light intensities in the cases where the LED light was passing through that had the same color (in other words, transmittance) as each part of the photomask were divided by the intensity detected without the films.

The gel sample was prepared in a petri dish (φ: 5 cm, the gel thickness: ~5 mm). At first, the photomask on the glass lid was covered on the petri dish, and 365-nm LED light (7.5 mW cm^{-2}) was irradiated to the gel sample through the photomask and lid from above for ~130 s (The writing process). After the writing process, the photomask and lid were removed, and then 365-nm LED light (6.1 mW cm^{-2}) was irradiated to the sample to read out the written information (The reading process). The read-out pattern was erased by the sol-gel transition: The gel sample was heated up to 55 °C on the hot plate and subsequently cooled at room temperature (The erasing process). The experiment under the condition with NaOH was conducted twice to record images and a movie, respectively.

Synthesis

Synthesis of the gelator (*N,N'*-bis(octadecyl)-l-Boc-glutamic diamide)

The gelator was synthesized according to the literature.[1] Boc-l-glutamic acid (0.645 g, 2.61 mmol) and octadecylamine (1.41 g, 5.23 mmol) were mixed in a 100 mL flask, and dichloromethane (50 mL) was added. Then 1-ethyl-3-(3-dimethylaminopropyl)carbodiimide hydrochloride (0.951 g, 5.20 mmol) and 1-hydroxybenzotriazole (0.704 g, 5.21 mmol) were added to the mixture, and the obtained mixture was stirred at room temperature for 68 hours. The obtained white solid was isolated by filtration and washed three times with dichloromethane. The crude product was dissolved in tetrahydrofuran and precipitated by water. A fine white solid was obtained (1.55 g, 77 % yield).

^{1}H-NMR (Chloroform-d/TMS, 400 MHz): δ 6.61 (s, 1H), δ 6.00 (s, 1H), δ 5.66 (s, 1H), δ 4.06 (m, 1H), δ 3.24 (m, 4H), δ 2.31 (m, 2H), δ 1.92–2.03 (m, 2H), δ 1.46–1.54 (m, 4H), δ 1.44 (s, 9H), δ 1.25 (br s, 60H), δ 0.88 (t, $J = 6.4$ Hz, 6H).
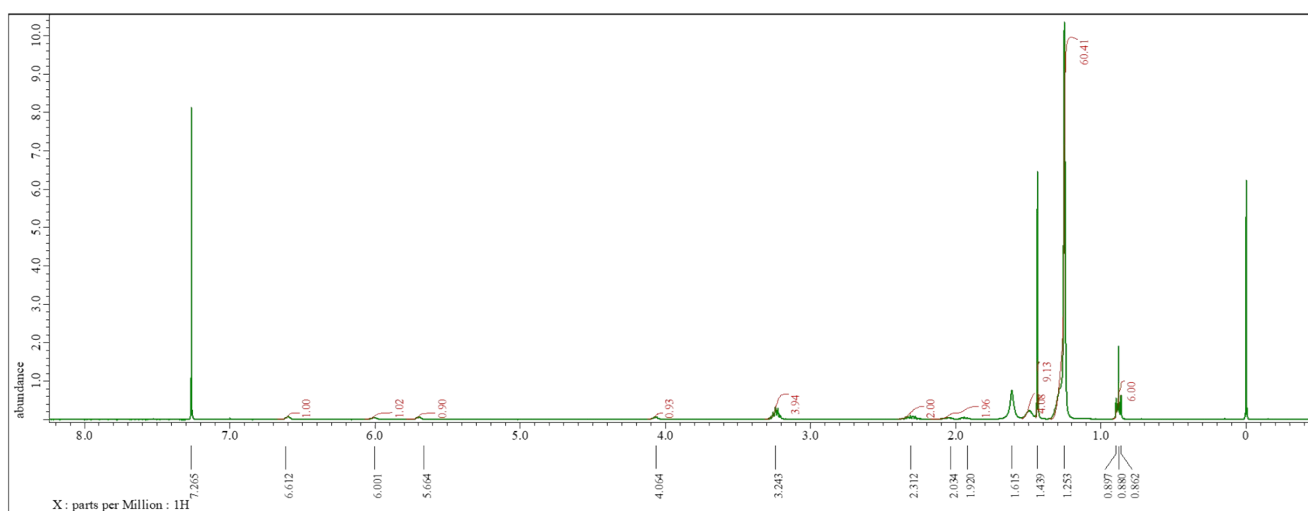

Fig. S1 ^{1}H-NMR spectrum of the gelator (Chloroform-d/TMS, 400 MHz).

Photoreduction of Anthraquinone in the Ethanol Solution
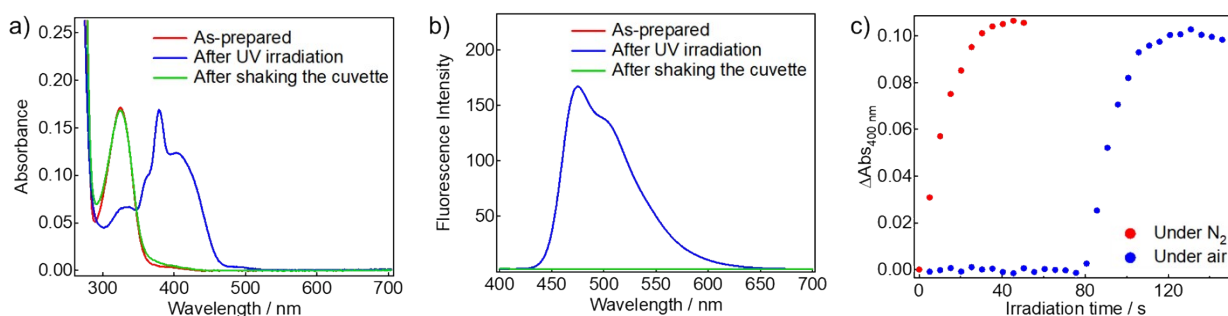

Fig. S2 a) Absorption and b) fluorescence (λ_{ex}: 365 nm) spectra of the air-saturated ethanol solution (400 μM AQ, 4 mM TEA, 1 mm cuvette) before and after UV irradiation (365 nm, 14.5 mW cm^{-2}) and air-oxidation. c) Coloration dynamics at 400 nm for the N$_2$-bubbled and air-saturated solutions upon continuous UV light irradiation.
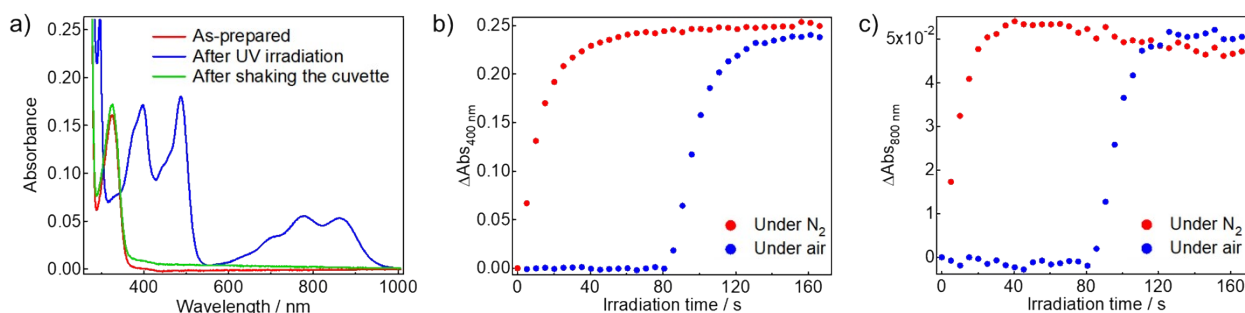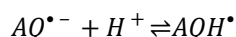

Fig. S3 a) Absorption spectra of the air-saturated ethanol solution containing 5 mM NaOH (400 μM AQ, 4 mM TEA, 1 mm cuvette) before and after UV irradiation (365 nm, 14.5 mW cm^{-2}) and air-oxidation. b,c) Coloration dynamics at (b) 400 and (c) 800 nm for the N$_2$-bubbled and air-saturated solutions upon continuous UV light irradiation.

According to the literature, AQ$^{\bullet-}$ in ethanol shows two sharp absorption bands at 398 and 488 nm and a broad absorption band centered at 776 nm, while AQ^{2-} in ethanol exhibits a sharp absorption band at 417 nm and a broad absorption band at 508 nm.[2] The absorption spectral shape shown in Fig. S3a blue is consistent with the characteristics of not AQ^{2-} but AQ$^{\bullet-}$, which indicates that the AQ$^{\bullet-}$ was obtained as the main product even in UV irradiation to AQ in the air-saturated ethanol added with NaOH.

As described in Fig. S9 and S10, photoexcitation of AQ in ethanol containing TEA produces AQ$^{\bullet-}$. According to the literature, AQ$^{\bullet-}$ is protonated to give AQH$^{\bullet}$, and the following disproportion of AQH$^{\bullet}$ generates AQH$_2$.[3]

$$2AQH^{\bullet} \rightarrow AQ + AQH_2$$

In alkaline solutions, however, AQH$^{\bullet}$ is expected to be a minor species based on the following equilibrium.

$$AQ^{\bullet-} + H^+ \rightleftharpoons AQH^{\bullet}$$

Therefore, coloration due to AQ$^{\bullet-}$ would be observed in ethanol added with NaOH.

Photoreduction of Anthraquinone in the Ethanol Gel without NaOH
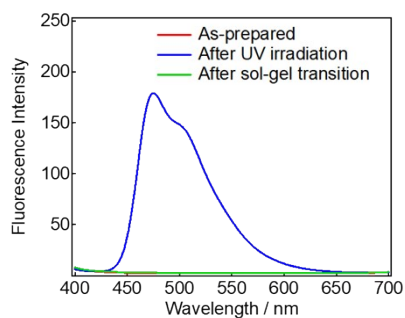

Fig. S4 Fluorescence spectra (λ_{ex}: 365 nm) of the air-saturated ethanol gel (400 μM AQ, 4 mM TEA, 1 mm cuvette) before and after UV light irradiation (365 nm, 14.5 mW cm^{-2}) and sol-gel transition.

Photoreduction of Anthraquinone in the Ethanol Gel with NaOH
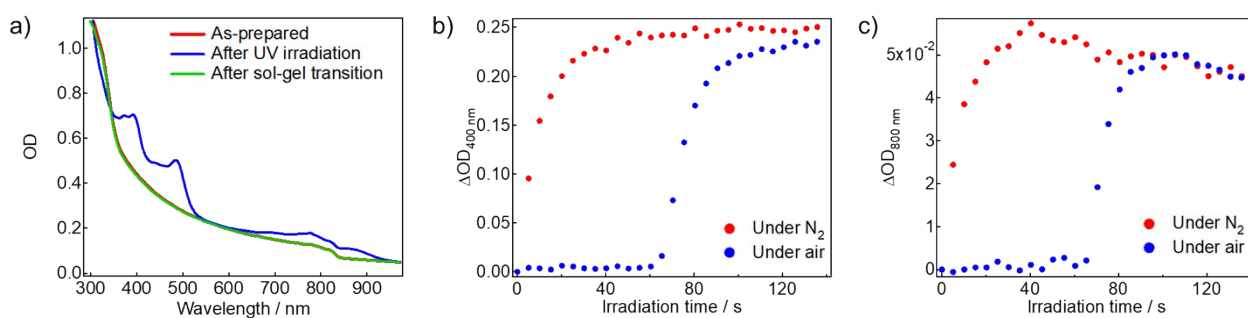

Fig. S5 a) Absorption spectra of the air-saturated ethanol gel containing 5 mM NaOH (400 μM AQ, 4 mM TEA, 1 mm cuvette) before and after UV irradiation (365 nm, 14.5 mW cm^{-2}) and sol-gel transition. b,c) Coloration dynamics at (b) 400 and (c) 800 nm for the N$_2$-bubbled and air-saturated gels upon continuous UV light irradiation.

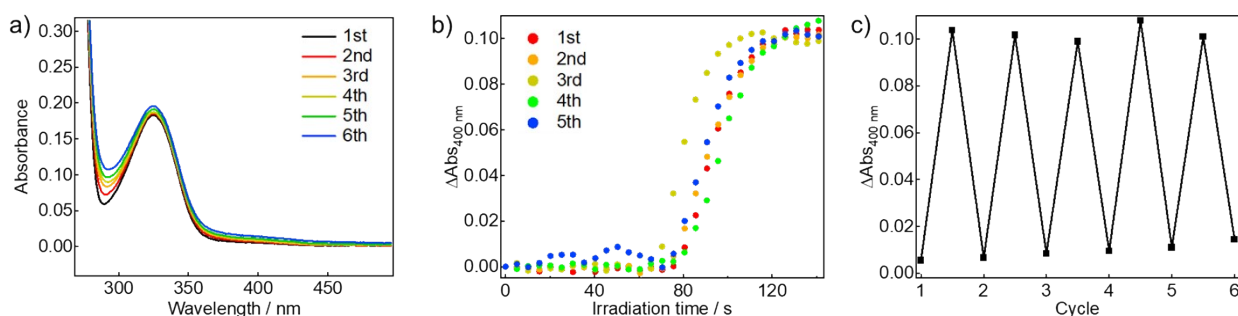## Cyclability of Photoreduction in the Ethanol Solution

Fig. S6 a) Absorption spectra of the air-saturated ethanol solution (400 μM AQ, 4 mM TEA, 1 mm cuvette) in each photoreduction-oxidation cycle before UV irradiation, b) Coloration dynamics at 400 nm during UV irradiation (365 nm, 14.5 mW cm^{-2}) in each cycle. c) Absorbance change at 400 nm by UV irradiation and air-oxidation in each cycle.

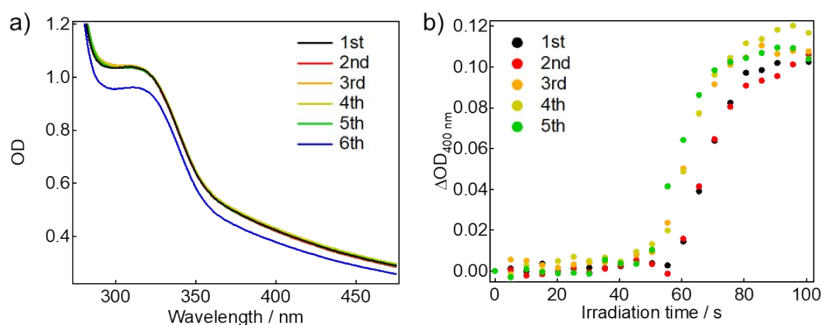## Cyclability of Photoreduction in the Ethanol Gel

Fig. S7 a) Absorption spectra of the air-saturated ethanol gel (400 μM AQ, 4 mM TEA, 1 mm cuvette) in each photoreduction-oxidation cycle before UV irradiation, b) Coloration dynamics at 400 nm during UV irradiation (365 nm, 14.5 mW cm^{-2}) in each cycle.

As shown in Fig. S6b and S7b, the coloration dynamics were slightly deviated in each cycle. The reason for this is probably that the dissolved oxygen concentration after the air-bubbling were not perfectly constant. Additionally, the absorption spectrum of the gel in 6th cycle was not overlapped on the other cycles (Fig. S7a). This is due to the fluctuation of the scattering owing to the gel.

UV Light Intensity Dependence of Coloration Dynamics in the Air-Saturated Gel
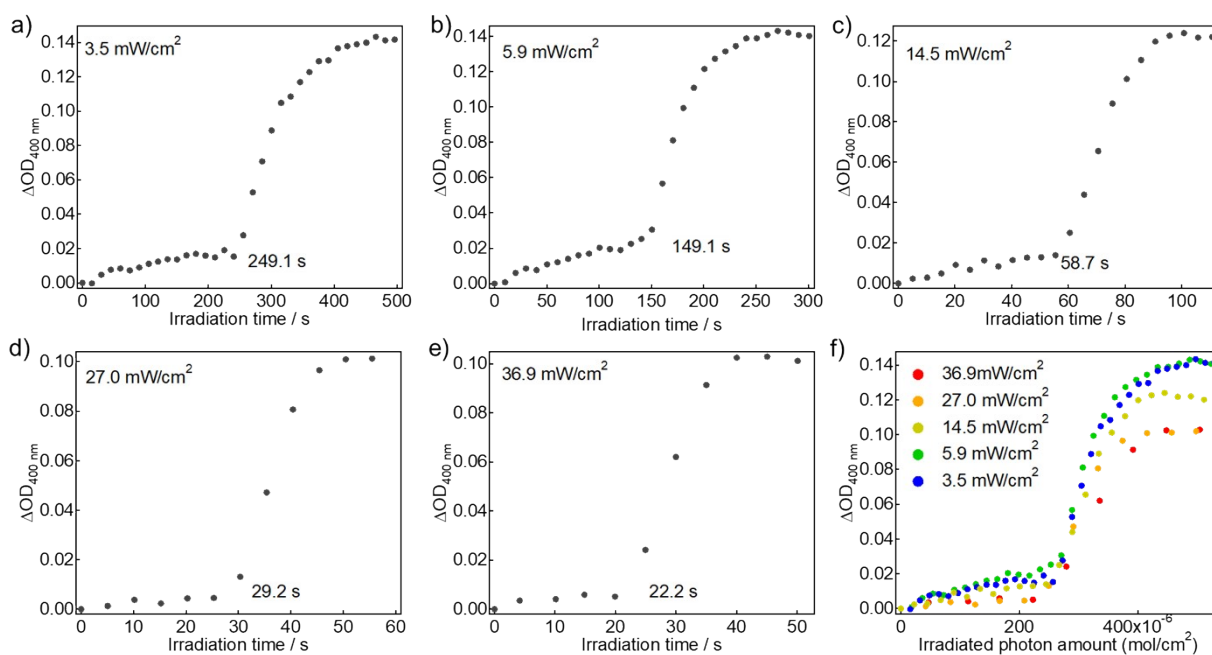

Fig. S8 a–e) Coloration dynamics at 400 nm and the induction periods for the air-saturated ethanol gel (400 μM AQ, 4 mM TEA, 1 mm cuvette) under different 365-nm light intensities (3.5–36.9 mW cm^{-2}); f) The dynamics plotted against the irradiated photon amount.

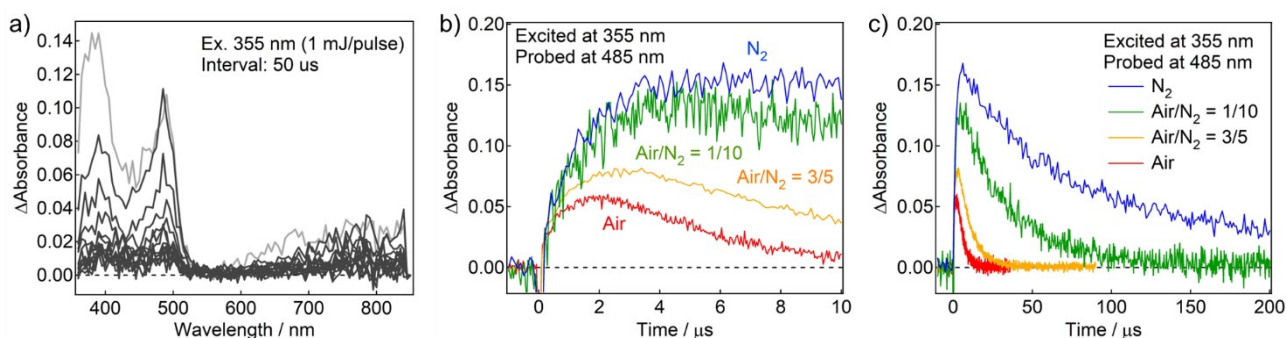# Transient Absorption Spectra of Anthraquinone in Ethanol Solution

Fig. S9 a) Microsecond transient absorption spectra under N_2 atmosphere and b,c) dynamics at 485 nm under various atmospheres of the ethanol solution (400 μM AQ, 4 mM TEA, 1 cm cuvette) excited at 355 nm (1 mJ/pulse).
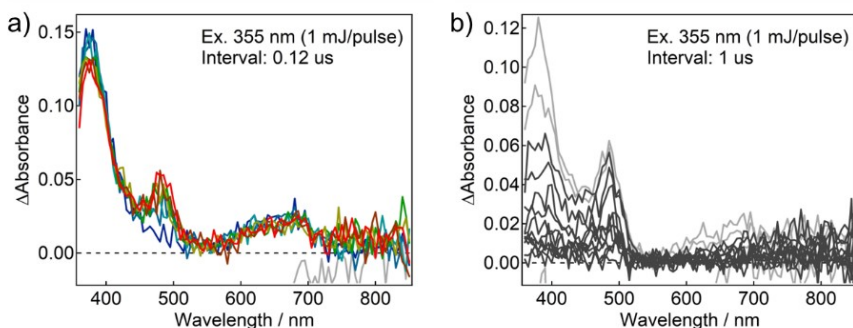

Fig. S10 a) Sub-microsecond and b) microsecond transient absorption spectra of the air-saturated ethanol solution (400 μM AQ, 4 mM TEA, 1 cm cuvette) excited at 355 nm (1 mJ/pulse).

To better understand which process in the photoreduction is influenced by the dissolved oxygen, we measured the transient absorption spectra of the solution sample using a 355-nm nanosecond pulse laser. First, in the N_2-bubbled solution, the rising of a positive signal at 485 nm was observed from immediately after excitation to several microseconds, and subsequently, the signal decayed over several hundreds of microseconds (Fig. S9a). According to the literature, the component showing the signal at 485 nm was assigned to the radical-ion pair $AQ^{\bullet-}–TEA^{\bullet+}$.[3] However, the literature reports that the radical-ion pair in the N_2 atmosphere exhibits little decay within several hundreds of microseconds, which indicates the potential for a small amount of oxygen to remain in our experiment. After the disappearance of the radical-ion pair, a residual signal was observed between 400–500 nm. Although this residual signal was weak and obscure, it might be attributed to any reduced form of AQ.

The air-saturated solution also exhibited transient spectral shapes, such as those in the N_2-bubbled solution, and a signal assigned to the radical-ion pair $AQ^{\bullet-}–TEA^{\bullet+}$ was observed at 485 nm. However, the rising and decay were much faster than those in the N_2-bubbled sample, and no residual components were detected in the air-saturated sample (Fig. S10a,b).

The transient absorption dynamics at 485 nm were compared by varying the bubbling gas composition (Fig. S9b,c). As the fraction of the air, i.e., the fraction of the oxygen increased, the decay was significantly faster. This result indicates that molecular oxygen took an electron from $AQ^{\bullet-}$ of the radical-ion pair to quench it. Moreover,

with respect to the signal rising, the rate increased and the maximal height decreased under conditions with more oxygen. This may indicate that molecular oxygen quenched precursors of the radical-ion pair: the T_1 state of AQ and the triplet exciplex formed by the reaction between the T_1 state and TEA. Therefore, we conclude that the dissolved oxygen quenches both the triplet excitons and the radical-ion pair under our experimental conditions. Importantly, the quenching occurred even in the low-oxygen concentration condition of Air/N_2 = 1/10, which indicates that practically, coloration by photoreduction progresses after the dissolved oxygen is almost finished.

Discussions on the Induction Period

The results in the coloration dynamics measurements under different atmospheres and light intensities, and the transient absorption measurements indicate the following equation showing the approximate relationship between the induction period t_i [s], the initial concentration of the dissolved triplet oxygen $[^3O_2]_0$ [mol L^{-1}], and the irradiation light intensity I [W cm^{-2}]:

$$t_i = \frac{[^3O_2]_0 \cdot 10^{-3} \cdot L}{N_p \cdot \phi_{cons}}$$

$$= \frac{E_p}{I \cdot (1 - 10^{-A})} \cdot \frac{[^3O_2]_0 \cdot 10^{-3} \cdot L}{\phi_{cons}}$$

$$= \frac{h \cdot c \cdot N_A}{I \cdot (1 - 10^{-A}) \cdot \lambda \cdot 10^{-9}} \cdot \frac{[^3O_2]_0 \cdot 10^{-3} \cdot L}{\phi_{cons}}$$

$$= \frac{[^3O_2]_0 \cdot L \cdot h \cdot c \cdot N_A \cdot 10^6}{I \cdot (1 - 10^{-A}) \cdot \phi_{cons} \cdot \lambda} \qquad (2)$$

where ϕ_{cons}, L, N_p, E_p, A, h, c, λ, and N_A denote the quantum yield for the consumption of molecular oxygen, the cuvette length [cm], the number of photons absorbed by AQ, the irradiation light energy [J mol^{-1}], the absorbance of AQ at the irradiated light wavelength, the Planck constant [J·s], the speed of light [m s^{-1}], the irradiated light wavelength [nm], and the Avogadro constant [mol^{-1}], respectively. Equation (1) in the manuscript is a simplified expression of Equation (2), and the constant K is given by the following equation:

$$K = \frac{L \cdot h \cdot c \cdot N_A \cdot 10^6}{\phi_{cons} \cdot \lambda} \qquad (3)$$

As shown by the transient absorption spectroscopy, the dissolved oxygen quenches quickly the intermediates in the photoreduction. Therefore, the concentration and absorbance of AQ remains almost constant during the induction period, and the oxygen consumption yield per irradiated photon is also constant. Consequently, a clock reaction-like behavior is observed, where the induction period is the period until the dissolved oxygen is finished (Fig. S11).

Considering the results of transient absorption spectroscopy, the dissolved oxygen quenches the T_1 state of AQ, its triplet exciplex with TEA, and the radical-ion pair. In the literature, the quantum yield of the photoreduction of AQ in N_2-purged ethanol containing 20 mM TEA was calculated as 0.92.[3] Because the photoreduction of AQ occurs via stepwise formation of the T_1 state, the exciplex with TEA, and the radical-ion pair, the quantum yield of each step should exceed 0.92. In such cases where the photoreduction quantum yield is nearly unity, the postulation that the quantum yields for the formation of the T_1 state, the exciplex, and the radical-ion pair are equal gives good simplification. All the quantum yields can be expressed by a single symbol ϕ_{form} because all the species can react with molecular oxygen. Now, supposing that the reactive oxygen species, which result from quenching the T_1 state, exciplex, and radical-ion pair of AQ, react with TEA and other chemical species to be consumed irreversibly with a single efficiency η_{cons}, ϕ_{cons} is denoted by the following equation:

$$\phi_{cons} = \phi_{form} \cdot \eta_{cons} \qquad (4)$$

Furthermore, from Equation (4), Equation (2) is transformed into the following equation:

$$t_i = \frac{[^3O_2]_0 \cdot l \cdot h \cdot c \cdot N_A \cdot 10^6}{I \cdot (1 - 10^{-A}) \cdot \phi_{form} \cdot \eta_{cons} \cdot \lambda} \quad (5)$$

If the photoreduction quantum yield under nitrogen atmosphere in our system is the same as in the literature, ϕ_{form} is set to 0.92.[3] According to the literature value of the oxygen concentration in air-saturated ethanol, $[^3O_2]_0$ is estimated as 2 mM.[4] When η_{cons} is set to 1, t_i in the standard experimental condition for the solution sample is calculated as ~250 s from Equation (5), and the theoretical value differs significantly from the experimental value (~80 s, Fig. S2c). To match the theoretical and experimental values, η_{cons} is required to be ~3.1. Although it initially appears incorrect that η_{cons} exceeds 1, the large value of η_{cons} can be understood as follows. First, when molecular oxygen quenches the triplet excitons and radical-ion pair, reactive oxygen species are generated to react mainly with TEA, and thereby other radical species such as carbon-centered radicals are produced.[5] These radical species probably show chain reactions with oxygen to contribute to the increase in η_{cons}.[6] Moreover, TEA$^{\bullet+}$, which results from the quenching of the radical-ion pair by oxygen, can also be involved in the chain consumption of oxygen.[7] Additionally, the dissolved oxygen concentration might differ slightly from the value in literature.

From a comparison of the air-saturated solution and gel, the induction period in the standard experimental condition was ~80 s in the solution and ~50 s in the gel (Fig. S2c, 2d). The reason for this remains unclear, but might be explained by the increase in the effective optical path length owing to multiple scattering in the gel,[8] and the inclusion of AQ, which is relatively solvophobic in ethanol, by the gel fibers.[9]
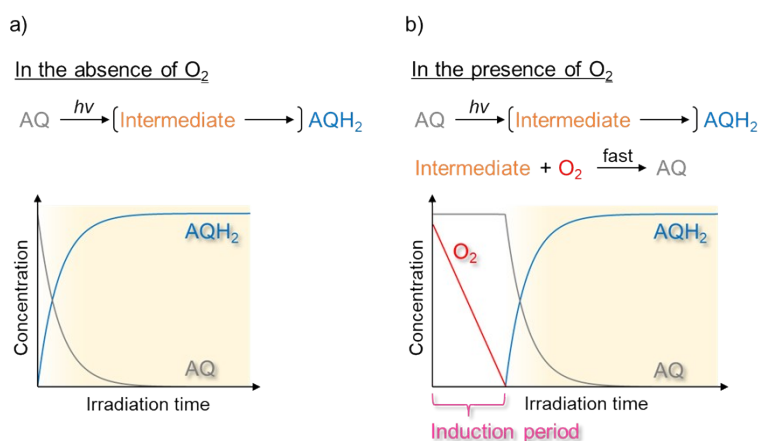

Fig. S11 Concentration change in the photoreduction of AQ to AQH$_2$; a) in the absence of O$_2$, b) in the presence of O$_2$.

Photoreduction of Anthraquinone in the Methanol Solution and Gel
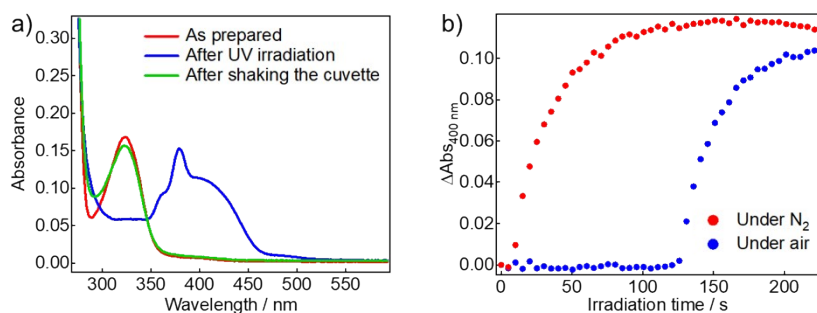

Fig. S12 a) Absorption spectra of the air-saturated methanol solution (400 μM AQ, 4 mM TEA, 1 mm cuvette) before and after UV irradiation (365 nm, 14.5 mW cm^{-2}) and air-oxidation. b) Coloration dynamics at 400 nm for the N$_2$-bubbled and air-saturated solutions upon continuous UV light irradiation.
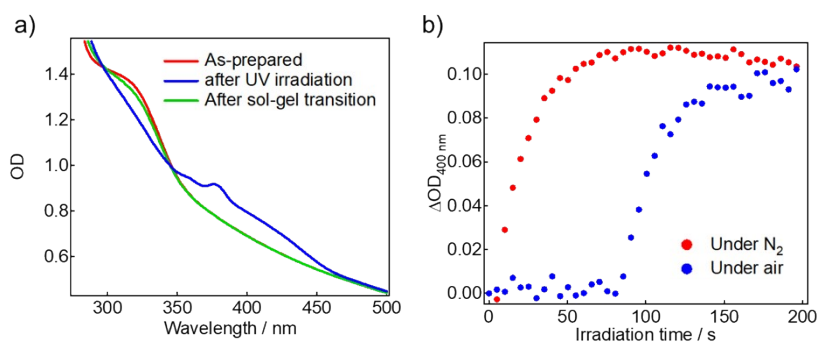

Fig. S13 a) Absorption spectra of the air-saturated methanol gel (400 μM AQ, 4 mM TEA, 6.7 mM gelator, 1 mm cuvette) before and after UV irradiation (365 nm, 14.5 mW cm^{-2}) and air-oxidation. b) Coloration dynamics at 400 nm for the N$_2$-bubbled and air-saturated gels upon continuous UV light irradiation.

When not ethanol but methanol was used as the solvent, the photoreduction of AQ progressed likewise, and the clock behavior was observed in the air-saturated solution and gel (Fig. S12, S13). In the solution under 365-nm LED light (Intensity: 14.5 mW cm^{-2}), the induction period was ~125 s (Fig. S10b). Assuming that ϕ_{form} is 0.92, similar to in ethanol,[4] and using 2 mM as the oxygen concentration in the air-saturated methanol according to the literature,[4] the equation (5) gave η_{cons} as ~1.5. This value is quite different from in ethanol, which indicates that η_{cons} is much influenced by the solvent.
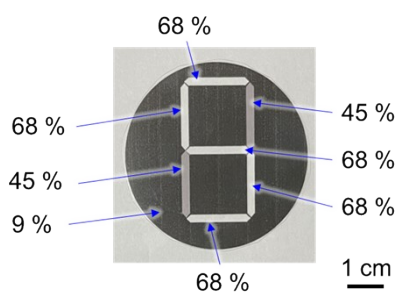
Spatiotemporal Photopatterning

Fig. S14 An image of the photomask and its transmittance at 365 nm.

References

1   Y. Li, T. Wang and M. Liu, *Soft Matter*, 2007, **3**, 1312–1317.

2   S. A. Carlson and D. M. Hercules, *Photochem. Photobiol.*, 1973, **17**, 123–131.

3   K. Hamanoue, T. Nakayama, Y. Yamamoto, K. Sawada, Y. Yuhara and H. Teranishi, *Bull. Chem. Soc. Jpn.*, 1988, **61**, 1121–1129.

4   M. Quaranta, M. Murkovic and I. Klimant, *Analyst*, 2013, **138**, 6243–6245.

5   R. S. Davidson and K. R. Trethewey, *J. Chem. Soc. Perkin Trans. 2*, 1977, 173–178.

6   M. G. Simic, *J. Chem. Educ.*, 1981, **58**, 125–131.

7   J. Hu, J. Wang, T. H. Nguyen and N. Zheng, *Beilstein J. Org. Chem.*, 2013, **9**, 1977–2001.

8   X. Zhou, J. Yu, L. Wang and Z. Zhang, *Appl. Opt.*, 2018, **57**, 3519–3523.

9   P. Duan, N. Yanai, H. Nagatomi and N. Kimizuka, *J. Am. Chem. Soc.*, 2015, **137**, 1887–1894.